Impacts of vesicular environment on Nox2 activity measurements in vitro

Xavier Serfaty, Pauline Lefrançois, Chantal Houée-Levin, Stéphane Arbault, Laura Baciou, Tania Bizouarn

Impacts of vesicular environment on Nox2 activity measurements *in vitro*

Xavier Serfaty[a], Pauline Lefrançois[b], Chantal Houée-Levin[a], Stéphane Arbault[b], Laura Baciou[a] and Tania Bizouarn[a]*

[a] Université Paris-Saclay, CNRS, Institut de Chimie Physique, UMR8000, 91405, Orsay, France ; [b] Univ. Bordeaux, ISM, CNRS UMR 5255, NSysA group, ENSCBP, 33607 Pessac, France.

*To whom correspondence should be addressed: Tania Bizouarn: Institut de Chimie Physique, Bat 350 Université Paris-Saclay, 91405 Orsay Cedex France; tania.bizouarn@universite-paris-saclay.fr; Tel. (+33) 1 6915 3016

Keywords: NADPH oxidase (NOX); cell-free assay; superoxide anion; cytochrome c reduction; oximetry

Highlights

- Vesicular context impacts Nox2 activity measurements
- Underestimation of Nox2 activity measurement from cytochrome *c* reduction
- $O_2^{\bullet-}$ and H_2O_2 disproportionation reactions arises in membrane neutrophils preparation

Abbreviations

The abbreviations used are: AA, *cis*-arachidonic acid; cyt b_{558}, cytochrome b_{558}; cyt *c*, cytochrome *c*; DOC, deoxycholate; DPI, diphenyl iodonium; DTT, dithiothreitol; MF, membrane fraction of neutrophil; NADPH, reduced β-nicotinamide adenine dinucleotide phosphate; Nox, NADPH oxidase; PBS, phosphate buffer saline; dPBS, Dulbecco phosphate buffer saline; PMSF, phenylmethanesulfonyl fluoride; SOD, superoxide dismutase.

ABSTRACT:

Background: The production of superoxide anions ($O_2^{\bullet-}$) by the phagocyte NADPH oxidase complex has a crucial role in the destruction of pathogens in innate immunity. Majority of *in vitro* studies on the functioning of NADPH oxidase indirectly follows the enzymatic reaction by the superoxide reduction of cytochrome *c* (cyt *c*). Only few reports mention the alternative approach consisting in measuring the NADPH consumption rate.

When using membrane vesicles of human neutrophils, the enzyme specific activity is generally found twice higher by monitoring the NADPH oxidation than by measuring the cyt *c* reduction. Up to now, the literature provides only little explanations about such discrepancy despite the critical importance to quantify the exact enzyme activity.

Methods: We deciphered the reasons of this disparity in studying the role of key parameters, including cyt *c* and arachidonic acid concentrations, in conjunction with an ionophore, a detergent and using Clark electrode to measure the O_2 consumption rates.

Results: Our results show that the $O_2^{\bullet-}$ low permeability of the vesicle membrane as well as secondary reactions ($O_2^{\bullet-}$ and H_2O_2 disproportionations) are strong clues to shed light on this inconsistency.

Conclusion and General Significance: These results altogether indicate that the cyt *c* reduction method underestimates the accurate Nox2 activity.

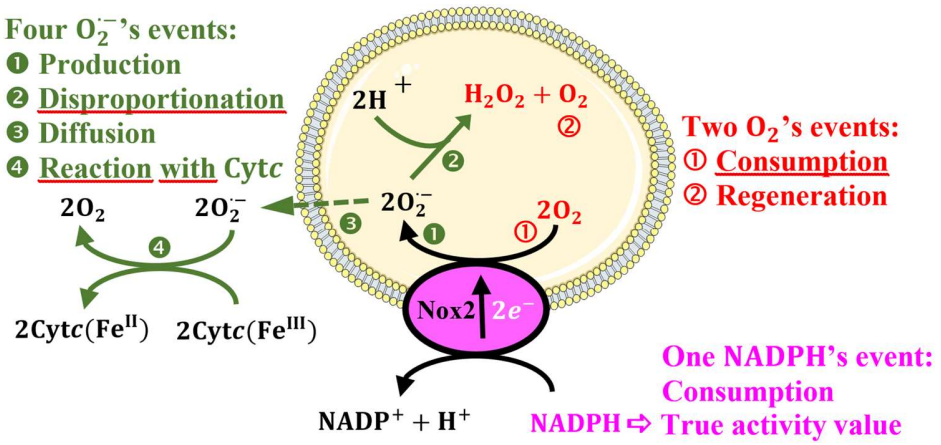

Graphical Abstract

INTRODUCTION:

The phagocyte NADPH oxidase has an essential function in the innate immune system (reviews [1,2]), in the destruction of pathogens due to a massive production of superoxide anions ($O_2^{\bullet-}$) in the phagosome [3]. This is called the oxidative burst. This enzyme is composed of two transmembrane proteins forming the flavocytochrome b_{558} (the catalytic core Nox2 and $p22^{phox}$), and four regulatory cytosolic proteins ($p40^{phox}$, $p47^{phox}$, $p67^{phox}$ and Rac1/2), that must bind to the dehydrogenase domain of Nox2 and $p22^{phox}$ to form an active complex (for reviews see [4-6]). In the resting state, neutrophils do not produce superoxide, the cytosolic proteins being distributed in the cytosol, alone or pre-assembled with some partners and the flavocytochrome b_{558} (cyt b_{558}) being in the plasma and granule membranes.

Superoxide anions production from dioxygen reduction using NADPH as electron donor is the sole catalytic function of NADPH oxidases. The substrate NADPH binds on the dehydrogenase domain of Nox2, delivers two electrons to the cofactor FAD that transfers them sequentially through two hemes to the final acceptors, two dioxygen molecules, on the other side of the membrane. The global reaction is:

$$NADPH + 2O_2 \rightarrow NADP^+ + H^+ + 2O_2^{\cdot-} \quad \text{(reaction 1)}$$

The phagocyte NADPH oxidase complex activity is studied in cell-free assays by mixing recombinant cytosolic proteins with native membrane fractions (MF), which are vesicles from the cell membrane of disrupted neutrophils. The system is activated by anionic amphiphilic molecules, commonly the all *cis*-arachidonic acid. The action of arachidonic acid consists in modifying the structure of most of the proteins of the complex [7,8] by enabling them to interact with each other and with phospholipids, resulting in the formation of an active enzyme [9-11]. In such cell-free assays, the enzyme activity is usually determined indirectly by measuring the rate of cytochrome *c* reduction by the produced superoxide anion [12]. Alternatively, measurement of the rate of NADPH oxidation is another approach to quantify the enzyme activity.

In the cell-free assay system used in this study, the catalytic core of the phagocyte NADPH oxidase is embedded in the plasma membrane of neutrophils. After disruption of this membrane, the membrane fraction (MF) consists in closed vesicles **[13,14]**. This membrane fraction contains vesicles with the NADPH oxidase oriented across the membrane in one direction and vesicles with the NADPH oxidase in the other orientation, unlike in phagosomes in which only the “inside-out” orientation occurs. The

cytosolic proteins and NADPH can only bind to the accessible dehydrogenase domain of Nox2, exposed to the external side of the MF vesicles. Thus, these vesicles are inside-out compared to plasma membrane. Consequently, the NADPH oxidation necessarily occurs on the outside of the MF vesicles and the superoxide anion production inside. This vesicular context can lead to difficulties to accurately measure the superoxide production. Indeed, the low permeability of membranes for negatively charged molecules such as $O_2^{\bullet-}$ leads to their sequestration, convoluted with side reactions such as superoxide disproportionation. According to reaction 1, in principle, the enzyme oxidizes one NADPH molecule to reduce two dioxygen molecules into two superoxide anions. Thus, the rate of superoxide production should be twice that of NADPH oxidation. However, experimentally, this is not the case and significant differences of this stoichiometry have been reported in literature [15-17]. Our aim with this paper is to elucidate these discrepancies. First, we identified what the cyt *c* approach really measures in order to evaluate the accuracy of the method for the determination of the initial rate of $O_2^{\bullet-}$ production by Nox-es. Second, we pointed out difficulties to get reliable enzymatic parameters from substrates or products quantifications.

MATERIAL AND METHODS

1 Materials

SP-Sepharose Fast-Flow (FF), Q-Sepharose-FF, Glutathione Sepharose-FF, and Ni-Sepharose-FF resins were purchased from GE-Healthcare-Bioscience. All *cis*-arachidonic acid, Dextran, phosphate buffer saline (PBS) Dulbecco PBS (dPBS), and equine heart cytochrome *c* were purchased from Sigma-Aldrich, and NADPH from ACROS.

The plasmids coding for the human cytosolic proteins, pET15b-Hisp67^{phox}, pET15b-Hisp47^{phox}, pGEX2T-GST-Rac1Q61L were provided by Dr. M.C. Dagher, Grenoble, France. All the plasmids were checked for their sequence by Beckman Coulter Genomics and used for transformation of *Escherichia coli* BL21(DE3).

2 Proteins purification

The production of the cytosolic proteins, Hisp67^{phox}, Hisp47^{phox} and GST-Rac1Q61L in transformed *E. coli* BL21(DE3) and their purification were realised as described in [18]. The protein solutions were then aliquoted and stored at -80°C. SDS-Page electrophoresis was performed during purification and the protein concentration estimated by absorbance at 280 nm using a Nanodrop™ spectrophotometer (Thermo Fisher, France).

3 Neutrophil membrane extraction

Fresh blood from healthy human donors was obtained from Etablissement Français du Sang (Cabanel-Paris, France). The neutrophils were purified following the protocol described in details in [18]. Neutrophil cells were broken by sonication and the suspension centrifuged 12 minutes at 10000 x g to remove organelles including granules and unbroken cells. The supernatant was centrifuged at 240000 x g for 90 minutes, the supernatant discarded and the pellets resuspended in the lysis buffer. The suspension of neutrophil membrane fraction was finally aliquoted and stored at -80°C. The cyt b_{558} concentration was estimated by diluting 100 µL of the suspension with 100 µL of dPBS + 1 % dodecyl maltoside. The absorbance at 411 nm and 427 nm was measured and the cyt b_{558} concentration was calculated from the ΔA ($A_{427\,nm}$ - $A_{411\,nm}$) using a differential extinction coefficient of 200 $cm^{-1}{\cdot}mM^{-1}$ [19].

4 NADPH oxidase activity measurements

Unless otherwise indicated, the following protocol was used. The membrane fractions (amount corresponding to 4 nM cyt b_{558}), 200 nM $p67^{phox}$, 200 nM $p47^{phox}$, 200 nM Rac1Q61L and AA were mixed together in this order in a 1 mL spectrophotometer cuvette containing PBS buffer supplemented with 10 mM $MgSO_4$. The mix was incubated 5 minutes at 25°C followed by addition of 200 µM NADPH to initiate the reaction. The activity was measured right after NADPH addition. Three methods were used to follow the NADPH oxidase activity: cytochrome *c* reduction by the produced superoxide, NADPH consumption and oxygen consumption. For activity measurement, the records were performed during one minute while for full time course of reactions records lasted up to one hour. The rates were estimated from the slope of the initial linear part of the curves. For easier comparison all activities have been plotted in graphs in "equivalent mol of $O_2^{\bullet-}$. sec^{-1}. mol of cyt $b_{558}{}^{-1}$". This means that the rate of NADPH oxidation have been multiplied by a factor 2.

- Cytochrome c reduction

The cyt *c* was added just before the incubation time and after the mixing of the whole cell-free assay components. The absorbance was followed at 550 nm using a spectrophotometer (Uvikon) for at least 1.5 minutes after NADPH addition. The differential extinction coefficient of the reduced *minus* oxidized state we used was $2.1{\cdot}10^4$ $cm^{-1}{\cdot}M^{-1}$ [20,21]. The rate of superoxide production should be theoretically equal to the cyt *c* reduction rate. In the case of complete kinetic studies, the end of the cyt *c* reduction was checked by addition of few grains of sodium-dithionite.

The dependence of Nox2 activity as a function of the cyt *c* concentration was measured as mentioned above with some adjustments. Because of the high used concentrations of cyt *c*, the path length of the cuvette was reduced to 1 mm. For an efficient mixing of the solution, the reaction mix was prepared in an Eppendorf tube incubated at 25°C in a water bath. NADPH was then added and the reaction mix rapidly

transferred in a thermostated quartz cuvette and the record of the absorbance changes at 550 nm was immediately started.

- NADPH oxidation

NADPH has a specific absorption band peak at 340 nm. The corresponding extinction coefficient used was 6200 $cm^{-1} \cdot M^{-1}$. The absorbance was followed for at least 1.5 minutes. The activities are not given as a function of NADPH reduced but as a function of the amount of electron transferred from NADPH per second per mol of $cytb_{558}$ to allow direct comparison with the other methods.

- Oxygen consumption

The oxygen consumption was measured using a Clark electrode (Oxygraph, Hansatech Instruments Ltd, UK). The vesicle membrane fractions, $p67^{phox}$, $p47^{phox}$, Rac1Q61L and AA were mixed together in a closed chamber under continuous stirring, thermostated at 25 °C and incubated at least 5 min. NADPH was then added and the variations of O_2 concentration followed as a function of time. After removal of all O_2 by nitrogen bubbling, the absence of O_2 intake from the outside has been verified during 14 h.

RESULTS

1 Nox2 activity assessed by cyt *c* reduction versus NADPH oxidation in standard conditions. *In vitro* Nox2 activity is commonly assessed by measuring the cyt *c* reduction rate by produced superoxide ions. The dependence of human Nox2 activity measured by this assay as a function of arachidonic acid (AA) concentration has a typical bell shape. It shows first an activation effect, up to 50 µM AA, followed by an inhibition effect for higher concentrations (Figure 1). The pattern of this bell shape may slightly vary with the origin of cells (*i.e.* the blood donor). In order to take into account the stoichiometry of NADPH to $O_2^{\bullet-}$ (reaction 1), values of NADPH consumption rates were multiplied by 2-fold. Although the oxidase activities measured by following the NADPH consumption also display a bell shape, the values were higher than those obtained from cyt *c* reduction rates. At the optimal AA concentration, the difference was at its maximum. Only for AA concentrations above 80 µM, rates displayed close values. The absence of activity in the absence of AA or of cytosolic proteins, indicates that the overestimation of NADPH oxidation is not coming from the presence of other NADPH-dependent enzymes. One should note that all the reactions were stopped by addition of diphenylene iodonium (DPI), a usual Nox enzyme inhibitor, confirming that kinetics were related to Nox2 enzyme activity. Cyt *c* reduction was stopped by addition of superoxide dismutase (SOD) showing that superoxide was effectively the molecule produced.

.

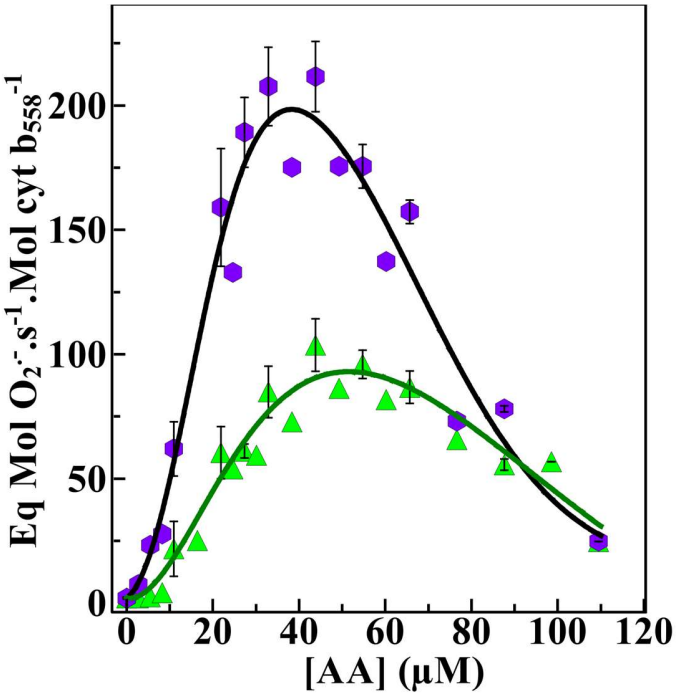

Figure 1. Dependence of Nox2 activity on AA concentration measured by cyt *c* reduction (green triangles) and NADPH oxidation (violet hexagons). The reaction was initiated by adding 200 µM NADPH. For cyt *c* measurements, reactions were performed in presence of 70 µM cyt *c*. Measurements were performed with a 5 min incubation time, as described in the material and methods section. The points are the mean ± the standard deviation of the results from 3 different membrane fractions (only some SD values are shown as examples). The curves are non-linearly fitted with a Simplex Nelder-Mead algorithm.

2 Relationship between cyt *c* concentration, cyt *c* reduction rate and superoxide production. Several explanations of the observed underestimation of the activity obtained with the cyt *c* reduction method can be proposed: slow superoxide diffusion through the membrane, cross-reaction(s) of superoxide with various targets possibly leading to other ROS and finally, lack of specificity of the probe itself.

The cyt *c* reduction measurement is a classic method to probe superoxide anions. It has been shown that in the case of superoxide produced in a non-compartmented system such as xanthine/xanthine oxidase, the cyt *c* reduction rate was equal to that of superoxide anion production. The rate constant for the reaction between superoxide anion and cyt *c* is expected to be about 10^6 M^{-1} s^{-1} at pH 7.2 [21-23] and the specific activity of the NADPH oxidase in usual conditions was measured to be around 100-200 Mol $O_2^{\cdot -}$. s^{-1} . (Mol cyt b_{558})$^{-1}$ [12], thus there should be no quantitative limitation by this method, 100% of superoxide should be scavenged by cyt *c*. We tested if the cyt *c* was at saturating concentrations towards the superoxide production by the NADPH oxidase. We followed the O_2 consumption during NADPH

oxidase activity as a function of cyt *c* concentration (Figure 2). If cyt *c* would be able to oxidize the totality of the superoxide formed, the total amount of dioxygen consumed should be recovered.

$$\text{cyt } c(Fe^{3+}) + O_2^{\cdot -} \rightarrow \text{cyt } c(Fe^{2+}) + O_2 \text{ (reaction 2)}$$

If we assume the rate of the reaction 1 is the limiting step, all O_2 consumed are recycled by reaction 2 thus no [O_2] variation is expected, as long as enough cyt *c*(Fe^{3+}) is available (Figure 2 dashed line). Instead, in presence of cyt *c*, the consumption of O_2 is a 2-phases kinetic (Figure 2) where O_2 is never totally recycled.

The duration and the slope of the first kinetic phase depend on the concentration of cyt *c*, whereas the second phase was cyt *c* concentration-independent.

In the first phase, the rate is the sum of reaction 2 (oxygen production) and reaction 1 (oxygen consumption). Even at the highest cyt *c* concentration (90 µM), the oxygen concentration decreased emphasizing that superoxide is not totally scavenged.

In the second phase, the three traces (red, green, blue) showed the same steeper slope. The oxygen consumption rate was then the same as in absence of cyt *c* (black trace), meaning the change of slope indicates that oxidized cyt *c* ended. This set of experiments clearly shows that cyt *c* at commonly used concentrations (*i.e.* <100 µM) can be considered as a limiting factor for oxidase activity measurements.

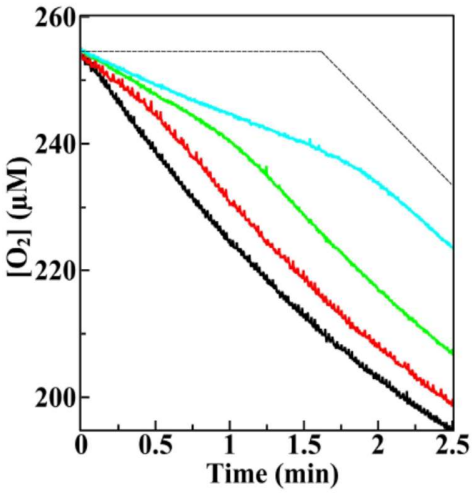

Figure 2. Evolution of O_2 concentration as a function of time for several cyt *c* concentrations. MF and cytosolic proteins were mixed in presence of 46 µM AA in PBS-$MgSO_4$ buffer. The reaction was triggered by addition of 200 µM NADPH. O_2 concentration evolution was measured as described in the material and methods section in presence of 0 µM cyt *c* (black), 23 µM cyt *c* (red), 45 µM cyt *c* (green)

and 90 μM cyt *c* (blue). The dashed line corresponds to the theoretical evolution of O_2 concentration in presence of 90 μM cyt *c* assuming that reaction 1 is limiting.

3 Determination of the kinetic parameters according to the detection method. We examined if the kinetic parameters (apparent catalytic constant k_{cat}^{app} and apparent Michaelis-Menten constant for NADPH K_m^{app}) may differ as a function of the detection method. Activities as a function of NADPH concentration were measured with three methods: by dioxygen uptake, NADPH oxidation and cyt *c* reduction for two different cyt *c* concentrations (50 μM and 360 μM). The data displayed a Michaelis-Menten behaviour as previously widely observed with the cyt *c* reduction approach [24]. The data fitting using the Michaelis-Menten equation leads to the estimation of k_{cat}^{app} and K_m^{app}, reported in Table 1 (curves in Supplementary Figure 1).

First, the k_{cat}^{app} corresponding to the two different cyt *c* concentrations are not similar. It confirms our previous result showing that usual cyt *c* concentration constitutes a limiting factor for superoxide detection. However, the apparent affinity constant of NADPH K_m^{app} is not significantly affected. In addition, the highest cyt *c* concentration (360 μM) leads to values very close to those of oxygen consumption measurements. Importantly, whatever the method employed to quantify the enzyme activity, the K_m^{app} values were in the same range. NADPH oxidation method gave again the highest value. This method being a direct measure of the activity, we can conclude that the O_2 uptake method leads to an underestimation of the activity as for that of cyt *c* reduction. Since K_m^{app} values were little affected, it means that the observed underestimation was not due to a limitation of the probe response (cyt *c*) or the Clark electrode response.

constants	NADPH oxidation	O_2 consumption	cyt *c* reduction 50 μM	cyt *c* reduction 360 μM
k_{cat}^{app} (s^{-1})	262 ± 10	239 ± 17	99 ± 6	213 ± 3
K_m^{app} (μM)	106 ± 11	158 ± 39	79 ± 16	98 ± 3

Table 1. Apparent catalytic k_{cat}^{app} and Michaelis-Menten constants for NADPH K_m^{app}. These values were obtained from different methods: NADPH oxidation, dioxygen consumption, cyt *c* reduction with cyt *c* concentration in default (50 μM) and cyt *c* reduction with cyt *c* concentration in excess (360 μM). Values were estimated from NADPH concentration dependence activities and given ± SEM.

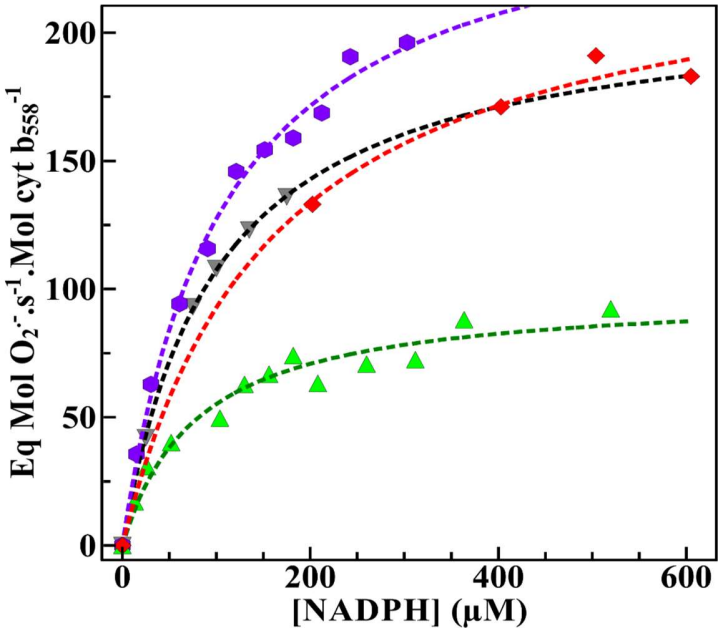

Supplementary Figure 1: Activity of Nox2 as a function of NADPH concentration. Reactions have been performed in presence of 4 nM cyt b_{558}, 200 nM of each $p67^{phox}$, $p47^{phox}$ and Rac1Q61L, 46 µM AA with an incubation time of 5 min at 25 °C. The NADPH oxidase activity has been measured at different NADPH concentrations from the cyt *c* reduction with 50 µM cyt *c* (green triangles), or with 360 µM cyt *c* (black inverted triangles), from dioxygen uptake measurements (red diamonds) and from NADPH oxidation measurements (violet hexagons). The optical path length was 1 cm, except in the case of 360 µM cyt *c* where a 1 mm path length cuvette was used as described in the Methods section. The fits were obtained from the Michaelis-Menten equation according to the values presented Table 1.

4 Importance of the incubation period on AA partition effects In cell-free assays, an incubation period of at least 5 minutes of the membrane fraction with the cytosolic proteins and AA is considered as an essential step for proper assembly of the NADPH oxidase complex. We measured the activity evolution by the cyt *c* reduction (550 nm) either without or with 10 min incubation time, or the NADPH oxidation (340 nm, without incubation time). This is illustrated herein (Figure 3) by the variations of the kinetic curves. For the cyt *c* reduction kinetics, after 10 min incubation time (dashed green line), the initial phase was linear, whereas without pre-incubation (plain green line), the initial phase followed first a sigmoidal shape, then displayed a linear phase, in agreement with previous works [25-27]. Surprisingly, no sigmoidal behaviours have ever been observed when the enzyme activity was monitored by measuring the NADPH

oxidation, even without incubation (blue line). This important observation suggests that the lag phase, observed for the cyt *c* reduction measurements with no incubation period relates to a limitation of the superoxide diffusion in addition to the possible role of the assembly and activation process of the NADPH oxidase complex.

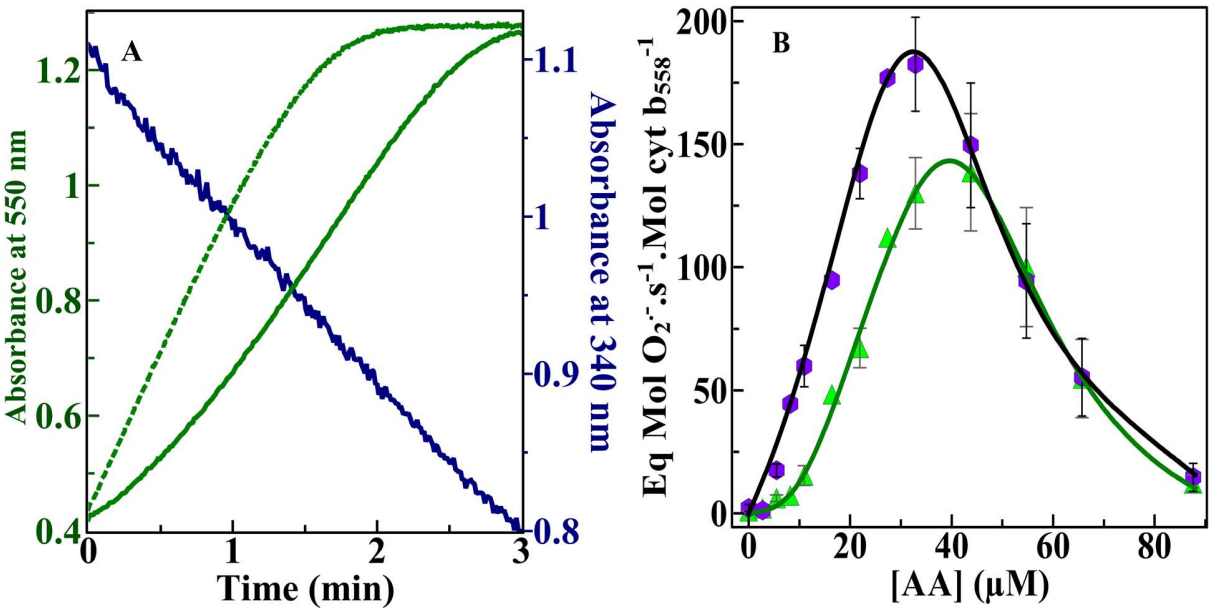

Figure 3. A: Cyt *c* reduction measured by absorbance at 550 nm (green, left axis) and NADPH oxidation measured at 340 nm (blue, right axis). Cyt *c* reduction was measured without incubation time (plain line) and with a 10 min incubation time (dashed line). NADPH oxidation was measured without incubation time. The reactions were performed in presence of 46 µM AA. The reaction was triggered by adding 174 µM NADPH. The cyt *c* reduction was obtained with 50 µM cyt *c*.

B: Effect of a 90 min-incubation period on activity dose-response curve to AA concentration. Activity of Nox2 as a function of arachidonic acid concentration from measurements of NADPH oxidation (violet hexagons) or cyt *c* (70 µM) reduction (green triangles) with an incubation period of 90 min instead of 5 min. The reaction was initiated by adding 200 µM NADPH. Values correspond to the mean ± the standard deviation of 3 independent measurements. The curves are non-linearly fitted with a Simplex Nelder-Mead algorithm.

In support to this idea, increasing the incubation time from 5 minutes (Figure 1) to 90 minutes (Figure 3B), brings the two curves closer, indicating that both methods are then better correlated. Instead of 80 µM AA necessary with a 5 minute-incubation period, only 40 µM were necessary to have a signal overlay for cyt *c* reduction and NADPH oxidation measurements. Our data definitely demonstrate that low AA concentrations or short incubation times lead to a bad coupling between reaction 1 and 2. We conclude

that membrane permeability for superoxide constitute a major limiting factor for the enzyme activity assay with cyt *c* measurement.

5 Impact of membrane permeability on activity measurements. We further investigated the impact of membrane permeability on activity measurements. Arachidonic acid is a good candidate to modify this parameter. By acting as a detergent on the membrane fractions of neutrophils, the arachidonic acid could help superoxide anions to cross the membrane and react with cyt *c* present outside the vesicles. Thus, we measured the oxidase activity with increasing concentrations of a detergent, deoxycholate (DOC) in the absence and presence of AA (46 µM) (Figure 4). The addition of DOC with AA led to a better correlation between the two methods, but mostly because of a faster decay of NADPH oxidation. Unfortunately, the gain on cyt c reduction measurement, due to an increase of superoxide diffusion, was partly lost by an inhibition of enzyme activity. This result is in good agreement with previous reports on the detergent effect such as DOC or Triton X-100 [16,17,28,29].

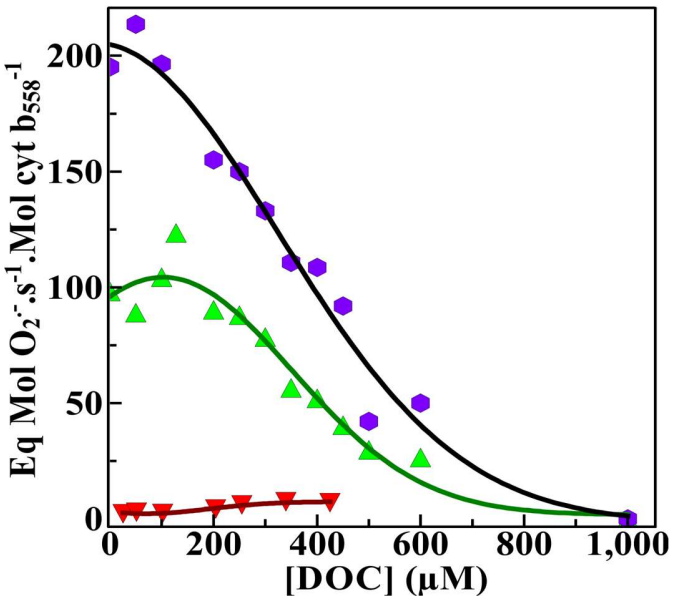

Figure 4. Effect of deoxycholate on the NADPH oxidase activity. Activity of Nox2 as a function of deoxycholate concentration measured in presence of 46 µM AA from NADPH oxidation (violet hexagons), cyt *c* (70 µM) reduction (green triangles) or cyt *c* (70 µM) reduction in absence of AA (red inverted triangles). DOC was added prior to the 5 min incubation time.

6 Disproportionation reactions during cell free assays

The main difference between the two methods used so far (NADPH oxidation *vs*. cyt *c* reduction) lies in the indirect activity measurement of the cyt *c* reduction method. Due to the compartmentalization in vesicles, the produced superoxide has to cross the membrane to be oxidized by cyt *c* outside the vesicle. The superoxide anion is unstable, due to its unpaired electron. The biochemical reactivity of this free radical is well described in literature [21,23]. In our system, the major side reaction is probably its spontaneous disproportionation (reaction 3).

$O_2^{\cdot -} + HO_2^{\cdot} + H^+ \rightarrow O_2 + H_2O_2$ ($k \approx 10^5$ $M^{-1} \cdot s^{-1}$ at pH 7.4) (reaction 3)

The disproportionation of superoxide anion is either spontaneous or enzymatically catalysed (SOD). To investigate the importance of this reaction in our system, the kinetic assays were recorded until total consumption of NADPH by absorbance spectroscopy at 550 and 340 nm (cyt *c* reduction and NADPH oxidation, respectively) (Figure 5A) and by oxygen consumption measurements using a Clark electrode (Figure 5B).

We first observed a fast increase in the absorbance signal at 550 nm during the first 3 min (Figure 5A plain line). The maximum absorbance value reached after 4 min indicates that the cyt *c* has been fully reduced. A slow decrease of the signal over 15 min revealed a slow re-oxidation of the reduced cyt *c*. The signal then reached a steady state. Importantly, the addition of NADPH 30 min after the first addition, again led to the total reduction of the oxidized cyt *c* available. It points out that the enzyme was still active. At 340 nm (Figure 5A dashed line), the signal progressively decreased over 20 min to reach an absorbance close to the baseline, indicating the NADPH was fully oxidized.

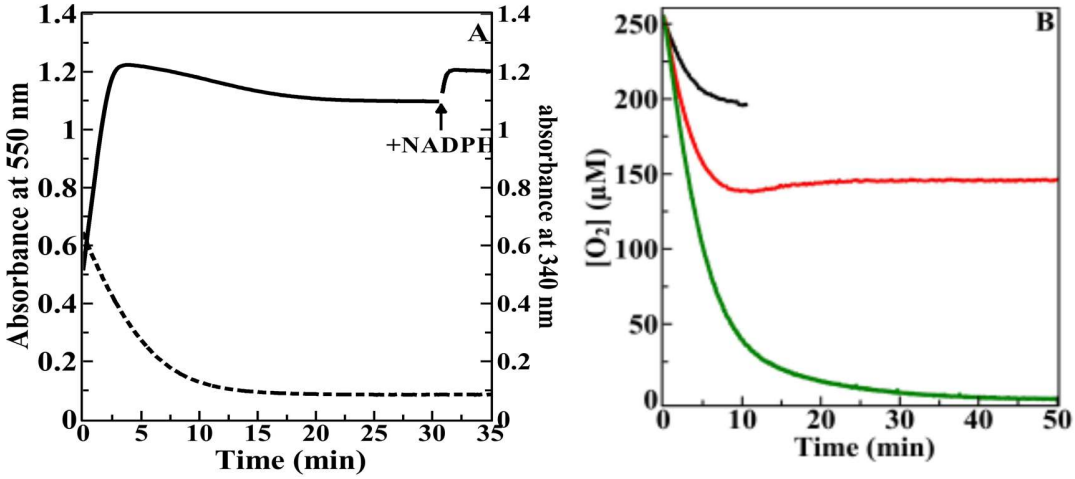

Figure 5. Time course of the reaction catalysed by the enzyme followed by (A) the NADPH oxidation (dashed line), the cyt *c* reduction (plain line) and (B) the O_2 consumption. Reactions were performed in presence of 46 µM AA as described in Method section. (**A**) Absorbance change at 550 nm was obtained in presence of 50 µM cyt *c*. The reaction was triggered by addition of 100 µM NADPH. The absorbance baseline at 340 nm was around 0.1. **(B)** O_2 concentration measurements using a Clark electrode for several NADPH concentrations: 100 µM NADPH (black), 200 µM NADPH (red) and 1.44 mM NADPH (green).

The re-oxidation of the reduced cyt *c* is due to the presence of an oxidant in solution, which is most likely the end product H_2O_2. Indeed, the addition of SOD at the maximum of cyt *c* reduction accelerated the cyt *c* re-oxidation (supplementary Figure 2).

In order to determine if the superoxide anion disproportionation reaction influenced our measurements, O_2 consumption measurements were performed using a Clark electrode (Figure 5B). If no disproportionation would occur, 100 or 200 µM NADPH consumption should correspond to an uptake of 200 or 400 µM O_2, respectively due to the reaction stoichiometry. In contrast, we observed that only 70 µM (black line) and 120 µM O_2 (red line) were consumed, for 100 and 200 µM NADPH respectively. In the presence of 1.44 mM NADPH, Nox2 could finally consume all O_2 present in the solution (green line). These results show that the disproportionation reactions occur at a time-scale equivalent to Nox2 reaction thus affecting our results. However, the superoxide disproportionation reaction had less impacted the O_2 consumption during the initial kinetic phase than the stationary phase of the reaction.

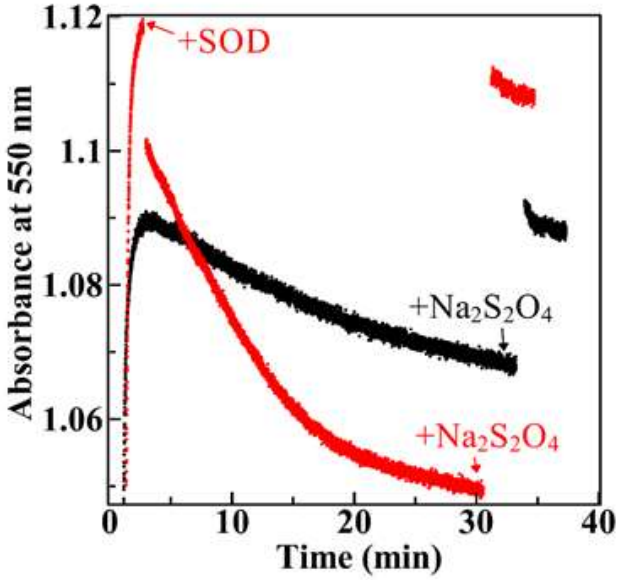

Supplementary Figure 2. Time dependence of cyt *c* reduction (550 nm) at the plateau in presence (red line) and absence (black line) of SOD. Reactions were performed in presence of 4 nM cyt b_{558}, 200 nM of each $p67^{phox}$, $p47^{phox}$, Rac1Q61L, 46 µM AA and 50 µM cyt *c* with an incubation time of 5 min at 25 °C. The reaction was triggered by addition of 100 µM NADPH. For the red curve, 50 units of superoxide dismutase were added at the maximum of the curve to convert the superoxide anion into H_2O_2. At 30 min, few grains of sodium dithionite ($Na_2S_2O_4$) were added to oxidize cyt *c*(Fe^{2+}) back to cyt *c*(Fe^{3+}).

Discussion

This study reveals a much more complex situation than it was first expected. Since the 1980s, the complicated regulation mechanism of Nox2 has been deciphered, the cofactors and cytosolic regulatory proteins have been identified, purifications of recombinant cytosolic proteins and the activation protocols have been established and improved. In general, in order to test the NADPH oxidase activity, the community felt safer to follow the SOD-inhibited production of superoxide indirectly by cyt *c* reduction rather than NADPH oxidation. However, the NADPH oxidation reflects directly the enzyme activity. The weakness of this latter lies on the limited NADPH concentration that can be used. Due to a loss of linearity in the absorbance signal above 1.5 for most routine spectrophotometers, it is very difficult to use saturating concentrations of NADPH. This can be resolved by shortening the optical pathlength. Although both methods display similar tendencies (shape of the curves as a function of the activator (AA), K_m^{app} for NADPH and the dependence on cytosolic factors), significant discrepancies in the results obtained with both methods have been observed [15-17]. Moreover, due to a lack of knowledge of the whole activation process, erroneous interpretations such as uncoupled enzymes or H_2O_2 production by Nox2 were

proposed. Here, our results confirm that the accuracy of Nox2 activity measured with the cytochrome *c* absorbance was not satisfying. This value depends on two major parameters: the diffusion of $O_2^{\bullet-}$ through the membrane and the rate of disproportionation reactions.

1 Membrane diffusion of $O_2^{\bullet-}$

The activity of the Nox2 enzyme seems to be dependent on its insertion into a membrane, or at least by the presence of phospholipids. For example, 40 mM of octyl glucoside leads to a total loss of activity that can be recovered by relipidation [30]. Therefore, in most cases, Nox2 is inserted in bilayer lipids membrane vesicles leading to a production of superoxide anions inside the vesicles, cyt c being located outside. With the production of $O_2^{\bullet-}$ occurring inside vesicles, it first has to diffuse through the membrane to reduce the cyt *c*. It has been shown that cyt *c* can interact with membrane components [31,32] and H_2O_2 [33]. At very high cyt *c* concentrations, we observed an increase in the cyt *c* reduction rate which is likely due to membrane perturbation by cyt c interactions [32]. This makes the encounter between cyt *c* and superoxide more likely due to an increase of the effective cyt *c* concentration at the membrane. These perturbations are unwanted for the study of Nox2 mechanism.

After a long incubation time in the presence of *cis*-arachidonic acid, a fatty acid known to activate the enzyme, we observed a better overlap between the bell-curves obtained with the NADPH oxidation and the cyt *c* reduction methods. This is likely due to increased membrane permeability. Consistently, the addition of detergent, such as DOC bring closer the results obtained with the cyt *c* reduction measurements to that obtained *via* the NADPH oxidation but it also had a strong inhibitory effect, which makes its use unreliable. Moreover, comparison of the kinetic curves with or without incubation (Figure 3), obtained with both spectroscopic methods, revealed that (i) AA-activation of the enzyme is indeed fast (< 1 min); (ii) the lag/sigmoidal part of the kinetic reports on the much slower effect of AA on the membrane (up to 90 min). These data suggest that in contrast to previous assumptions, incubation period does not relate strictly to NADPH oxidase activation step, which is *in fine* immediate in the timescale of *in-vitro* assay, but rather correspond to the time needed to render the membrane porous to superoxide. This brings clues to differences observed in different works based on neutrophils from different species, or on different phagocyte cell types.

2 Disproportionation reactions

The O_2 consumption rate measurement with Clark electrode has several disadvantages: a long initial equilibration period (electrode polarization) is needed for each measurement before the addition of NADPH and significant drifts of the signal are often present. However, even if this technique is not convenient enough to be used as a routine quantitative measurement, it helped us high-lightened disproportionation reactions (Figure 5B). Interestingly, as seen [34], the system appears to consume much

less O_2 than it should do: upon addition of 200 µM NADPH (Figure 5B), we detected that less than 120 µM dioxygen has been consumed instead of the 400 µM expected. Even if O_2 is partially recycled by superoxide anion disproportionation, this would only explain 70 % (200 µM) of the amount of O_2 regenerated (280 µM). As for the disappearance of H_2O_2, myeloperoxidases are good candidates since they are very abundant in neutrophils [35] and their characteristic absorbance peaks are slightly visible on the absorbance spectra of the membrane fractions of our neutrophils and others [16,36], however they do not form dioxygen. Thus, we can assume that membrane bound catalase-like enzyme may also be present to explain the observed inconsistency (as suggested by preliminary experiments). Indeed, by comparing the rates measured with the three methods, we could reach information on the relative contribution of each reactions in the whole system. First, the difference between the O_2 consumption rate and the cyt *c* reduction rate comes from the superoxide diffusion limitation through the membrane. Secondly, the difference between the NADPH oxidation rate and the O_2 consumption rate corresponds to the reformation of O_2 by the disproportionation reactions. The amplitude of cyt *c* reduction rate indicates that the rate of $O_2^{\bullet-}$ disproportionation inside the vesicle is in the same order or lower than the rate of permeation through the membrane. In the case of a faster disproportionation reaction than diffusion rates, it would have been impossible to see any reduction of cyt *c* by $O_2^{\bullet-}$.

3 Conclusion

These results altogether indicate that the cyt *c* reduction method underestimates the true Nox2 activity especially at short incubation times in a vesicle context. Nevertheless, this method is a good semi-quantitative tool to check the relative production of the end enzymatic product, the superoxide anion. Due to compartmentation, superoxide anions first have to diffuse through the membrane before being able to react with cyt *c*. In such a system, diffusion and disproportionation competes. Since cyt *c* can be reduced, it is likely that the rates of the disproportionation reactions are in the same order or slower than the $O_2^{\bullet-}$ diffusion through the membrane. The disproportionation rates are yet still fast enough to affect the activity measurements. Finally, the detergent-like property of AA acts is essential to increase the membrane permeability to anions but this effect is a slow process. All these issues could be circumvented by privileging the measurement of NADPH oxidation. This is even more justified while searching for inhibitors, since cyt *c* can also be reduced and superoxide anion can be oxidized by diverse molecules [37].

FUNDING

This work was supported by Electricité de France, Grant RB 2016-21.

REFERENCES

[1] Grandvaux, N., Soucy-Faulkner, A. and Fink, K. (2007). Innate host defense: Nox and Duox on phox's tail. Biochimie 89, 1113-22.

[2] Leto, T.L. and Geiszt, M. (2006). Role of Nox family NADPH oxidases in host defense. Antioxid Redox Signal 8, 1549-61.

[3] DeLeo, F.R., Allen, L.A., Apicella, M. and Nauseef, W.M. (1999). NADPH oxidase activation and assembly during phagocytosis. J Immunol 163, 6732-40.

[4] Groemping, Y. and Rittinger, K. (2005). Activation and assembly of the NADPH oxidase: a structural perspective. Biochem J 386, 401-16.

[5] Cross, A.R. and Segal, A.W. (2004). The NADPH oxidase of professional phagocytes--prototype of the NOX electron transport chain systems. Biochim Biophys Acta 1657, 1-22.

[6] Sumimoto, H. (2008). Structure, regulation and evolution of Nox-family NADPH oxidases that produce reactive oxygen species. FEBS J 275, 3249-77.

[7] Swain, S.D., Helgerson, S.L., Davis, A.R., Nelson, L.K. and Quinn, M.T. (1997). Analysis of activation-induced conformational changes in p47phox using tryptophan fluorescence spectroscopy. The Journal of biological chemistry 272, 29502-10.

[8] Bizouarn, T. et al. (2017). Exploring the arachidonic acid-induced structural changes in phagocyte NADPH oxidase p47(phox) and p67(phox) via thiol accessibility and SRCD spectroscopy. The FEBS journal 283, 2896-910.

[9] Pick, E. (2020). Using Synthetic Peptides for Exploring Protein-Protein Interactions in the Assembly of the NADPH Oxidase Complex. Methods Mol Biol 1982, 377-415.

[10] Matono, R., Miyano, K., Kiyohara, T. and Sumimoto, H. (2014). Arachidonic acid induces direct interaction of the p67(phox)-Rac complex with the phagocyte oxidase Nox2, leading to superoxide production. J Biol Chem 289, 24874-84.

[11] Shiose, A. and Sumimoto, H. (2000). Arachidonic acid and phosphorylation synergistically induce a conformational change of p47phox to activate the phagocyte NADPH oxidase. The Journal of biological chemistry 275, 13793-801.

[12] Pick, E. (2014) Cell-free NADPH oxidase activation assays: "in vitro veritas". In Methods in molecular biology (Clifton, N J) (Quinn, M.T. and DeLeo, ed.^eds), pp. 339-403

[13] Borregaard, N., Heiple, J.M., Simons, E.R. and Clark, R.A. (1983). Subcellular localization of the b-cytochrome component of the human neutrophil microbicidal oxidase: translocation during activation. J Cell Biol 97, 52-61.

[14] Klempner, M.S., Mikkelsen, R.B., Corfman, D.H. and Andre-Schwartz, J. (1980). Neutrophil plasma membranes. I. High-yield purification of human neutrophil plasma membrane vesicles by nitrogen cavitation and differential centrifugation. J Cell Biol 86, 21-8.

[15] Sha'ag, D. (1989). Sodium dodecyl sulphate dependent NADPH oxidation: an alternative method for assaying NADPH-oxidase in a cell-free system. J Biochem Biophys Methods 19, 121-8.

[16] Light, D.R., Walsh, C., O'Callaghan, A.M., Goetzl, E.J. and Tauber, A.I. (1981). Characteristics of the cofactor requirements for the superoxide-generating NADPH oxidase of human polymorphonuclear leukocytes. Biochemistry 20, 1468-76.

[17] Green, T.R. and Wu, D.E. (1986). The NADPH:O2 oxidoreductase of human neutrophils. Stoichiometry of univalent and divalent reduction of O2. J Biol Chem 261, 6010-5.

[18] Bizouarn, T., Souabni, H., Serfaty, X., Bouraoui, A., Masoud, R., Karimi, G., Houee-Levin, C. and Baciou, L. (2019). A Close-Up View of the Impact of Arachidonic Acid on the Phagocyte NADPH Oxidase. Methods in molecular biology (Clifton, N J) 1982, 75-101.

[19] Pick, E., Bromberg, Y., Shpungin, S. and Gadba, R. (1987). Activation of the superoxide forming NADPH oxidase in a cell-free system by sodium dodecyl sulfate. Characterization of the membrane-associated component. The Journal of biological chemistry 262, 16476-83.

[20] van Gelder, B. and Slater, E.C. (1962). The extinction coefficient of cytochrome c. Biochim Biophys Acta 58, 593-5.
[21] Bielski, B. (1978). Reevaluation of the spectral and kinetic properties of HO2 and O2- free radicals. Photochemistry and photobiology 28, 645-649.
[22] Butler, J., Jayson, G.G. and Swallow, A.J. (1975). The reaction between the superoxide anion radical and cytochrome c. Biochim Biophys Acta 408, 215-22.
[23] Bielski, B., Cabelli, D., Arudi, R. and Ross, A. (1985). Reactivity of HO2/O2- radicals in aqueous solution. J. Phys. Chem. 14(4), 1041-1099.
[24] Baciou, L., Erard, M., Dagher, M.-C. and Bizouarn, T. (2009). The cytosolic subunit p67phox of the NADPH-oxidase complex does not bind NADPH. FEBS letters 583, 3225-9.
[25] Karimi, G., Houee Levin, C., Dagher, M.C., Baciou, L. and Bizouarn, T. (2014). Assembly of phagocyte NADPH oxidase: A concerted binding process? Biochimica et biophysica acta 1840, 3277-83.
[26] Babior, B.M., Kuver, R. and Curnutte, J.T. (1988). Kinetics of activation of the respiratory burst oxidase in a fully soluble system from human neutrophils. J Biol Chem 263, 1713-8.
[27] Cross, A.R., Erickson, R.W. and Curnutte, J.T. (1999). Simultaneous presence of p47(phox) and flavocytochrome b-245 are required for the activation of NADPH oxidase by anionic amphiphiles. Evidence for an intermediate state of oxidase activation. J Biol Chem 274, 15519-25.
[28] Babior, G.L., Rosin, R.E., McMurrich, B.J., Peters, W.A. and Babior, B.M. (1981). Arrangement of the respiratory burst oxidase in the plasma membrane of the neutrophil. J Clin Invest 67, 1724-8.
[29] Wakeyama, H., Takeshige, K., Takayanagi, R. and Minakami, S. (1982). Superoxide-forming NADPH oxidase preparation of pig polymorphonuclear leucocyte. Biochem J 205, 593-601.
[30] Shpungin, S., Dotan, I., Abo, A. and Pick, E. (1989). Activation of the superoxide forming NADPH oxidase in a cell-free system by sodium dodecyl sulfate. Absolute lipid dependence of the solubilized enzyme. J Biol Chem 264, 9195-203.
[31] Tuominen, E.K.J., Wallace, C.J.A. and Kinnunen, P.K.J. (2002). Phospholipid-cytochrome c interaction: evidence for the extended lipid anchorage. The Journal of biological chemistry 277, 8822-6.
[32] Subramanian, M., Jutila, A. and Kinnunen, P.K. (1998). Binding and dissociation of cytochrome c to and from membranes containing acidic phospholipids. Biochemistry 37, 1394-402.
[33] Turrens, J.F. and McCord, J.M. (1988). How relevant is the reoxidation of ferrocytochrome c by hydrogen peroxide when determining superoxide anion production? FEBS Lett 227, 43-6.
[34] Green, T.R. and Shangguan, X. (1993). Stoichiometry of O2 metabolism and NADPH oxidation of the cell-free latent oxidase reconstituted from cytosol and solubilized membrane from resting human neutrophils. J Biol Chem 268, 857-61.
[35] Nauseef, W.M. (2014). Myeloperoxidase in human neutrophil host defence. Cell Microbiol 16, 1146-55.
[36] Doussière, J., Gaillard, J. and Vignais, P.V. (1996). Electron transfer across the O2- generating flavocytochrome b of neutrophils. Evidence for a transition from a low-spin state to a high-spin state of the heme iron component. Biochemistry 35, 13400-10.
[37] Jaquet, V., Scapozza, L., Clark, R.A., Krause, K.H. and Lambeth, J.D. (2009). Small-molecule NOX inhibitors: ROS-generating NADPH oxidases as therapeutic targets. Antioxid Redox Signal 11, 2535-52.